https://doi.org/10.5194/wes-2019-88
Preprint. Discussion started: 2 December 2019

WIND ENERGY SCIENCE DISCUSSIONS

Differences in damping of edgewise whirl modes operating an upwind turbine in a downwind configuration

Gesine Wanke[1], Leonardo Bergami[1], and David Robert Verelst[2]

[1]Suzlon Blade Science Center, Havneparken 1, 7100 Vejle, Denmark
[2]DTU Wind Energy, Technical University of Denmark, Frederiksborgvej 399, 4000 Roskilde, Denmark

Correspondence: Gesine Wanke (gesine.wanke@suzlon.com)

Abstract. The qualitative changes in damping of the first edgewise modes when an upwind wind turbine is converted into the respective downwind configuration are investigated. A model of a Suzlon S111 2.1MW turbine is used to show that the interaction of tower torsion and the rotor modes is the main reason for the change in edgewise damping. For the forward whirl mode a maximum decrease in edgewise damping of 39% is observed and for the backward whirl mode a maximum increase of 18% in edgewise damping is observed when the upwind configuration is changed into the downwind configuration. The shaft length is shown to be influencing the interaction between tower torsion and rotor modes as out-of-plane displacements can be increased or decreased with increasing shaft length due to the phase difference between rotor and tower motion. Modifying the tower torsional stiffness is seen to give the opportunity in the downwind configuration to account for both, a favorable placements of the edgewise frequency relative to the second yaw frequency, as well as a favorable phasing in the mode shapes.

1 Introduction

Upwind wind turbines, where the rotor is placed in front of the tower relative to the wind, have been in the focus of research efforts for the recent years. As wind turbines increase in size, and cost of energy has to be reduced, rotor blades become longer and increase in flexibility. The blade tip to tower clearance is a constraint for the design of such blades. Downwind rotors, where the rotor is placed behind the tower are not subject to such constraint during normal operation and re-experience therefore an increase in research effort.

The downwind concepts are known to show a higher fatigue load for the flapwise blade root moments compared to the upwind concepts due to the tower shadow effect. Glasgow et al. (1981) measured a significant fatigue load increase in the flapwise bending loads for a downwind configuration compared to an upwind configuration of a 100kW machine due to the velocity deficit of a truss tower. Zahle et al. (2009) simulated a reduction in normal force on the blade of 20%, due to the rapid fluctuation in the angle of attack as the blade passes through the tower wake. A fatigue load increase of around 20% for the damage equivalent flapwise blade root bending moment was found by Reiso and Muskulus (2013), when comparing the 5MW NREL

https://doi.org/10.5194/wes-2019-88
Preprint. Discussion started: 2 December 2019

eawe european academy of wind energy
Open Access WIND ENERGY SCIENCE DISCUSSIONS

reference turbine in a downwind configuration to the original upwind configuration.

A comparison of a full design load basis for a commercial Suzlon class IIIA 2.1MW wind turbine in an upwind configuration and a downwind configuration by Wanke et al. (2019) showed, that also the edgewise fatigue load increases significantly, when changing the upwind configuration into a downwind configuration. Only 30% of the fatigue load increase for the edgewise blade root sensor could be associated with the tower shadow effect. The remaining fatigue load increase could be associated with a lower edgewise damping in the foreward whirl mode of the downwind configuration.

In the 1990s first research efforts were made to characterize the damping of the edgewise blade modes since some stall regulated turbines showed stall induced vibrations. Petersen et al. (1998a) described how the local edgewise vibrations coupled to the substructure in global foreward (FW) and backward (BW) whirling modes. The whirling modes resulted into a force at the hub center, rotating either with the rotational direction of the shaft (FW) or against the rotational direction of the shaft (BW). Energy was seen to be exchanged between the blade and rotor modes if the frequencies were placed close together. Lower damping of the modes was shown to lead to a significant increase in both fatigue and extreme loads as vibration amplitudes are higher.

In the 'STALLVIB'-project Petersen et al. (1998b) aimed to predict margins of damping, identify important parameter influencing the edgewise damping and to establish design guidelines to prevent the occurrence of stall induced vibrations. It was seen that the aerodynamic damping determined if stall induced vibrations would occur. Out-of plane motion could generally be associated with higher aerodynamic damping. Airfoil characteristics such as the stall behaviour and the slope of the lift curve over the angle of attack were found to determine if the aerodynamic force created from the vibration velocity restored the steady state position.

Thomsen et al. (2000) used a rotating mass on the nacelle to excite the edgewise whirling modes for a 600kW upwind turbine. From the measured blade root moment the damping for the edgewise whirling modes was calculated. The results showed that the edgewise foreward whirling mode was significantly higher damped than the corresponding backward whirling mode.

Hansen (2003) build a linearized model with 15 degrees of freedom to determine the damping for the edgewise modes of the turbine, measured by Thomsen et al. (2000), using an eigenvalue approach. Hansen could confirm that the edgewise foreward whirl mode was significantly higher damped than the edgewise backward whirl mode. From the visualization of the modal amplitudes it could be shown that the edgewise foreward whirl mode had a significant higher out-of-plane component than the backward whirl mode, contributing positively to the damping. The work recommended that the over all edgewise damping could be significantly increased, if the turbine design was able to place the edgewise blade frequency between the 2nd yaw and tilt frequency of the turbine, as this increased the out-of plane contribution of the edgewise foreward whirl mode.

In the description of aeroelastic instabilities Hansen (2007) derived the aerodynamic damping coefficient of a single airfoil in dependency on the vibration direction. From the simplified analysis he was able to show how the aerodynamic damping relates to the inflow velocity, the airfoil coefficients and the airfoil coefficient slopes over the angle of attack for different quadrants of vibration direction.

This paper will focus on the difference in edgewise damping when the Suzlon S111 2.1MW wind turbine is changed from an upwind configuration into a downwind configuration. The damping of the edgewise whirl modes will be estimated from

https://doi.org/10.5194/wes-2019-88
Preprint. Discussion started: 2 December 2019

timeseries for the two turbine configurations and different sets of flexibility in the components. Finally, shaft length, cone angle and tower torsion are varied to show how the edgewise damping could be influenced by the turbine design.

The interaction of the rotor and the tower torsion will be shown to cause differences in the maximum damping between the two edgewise whirl modes and the two turbine configurations. The interaction of the edgewise foreward whirl mode and the tower torsion increases the edgewise damping in the upwind configuration and decreases the edgewise damping in the downwind configuration. In the foreward whirl mode the edgewise damping decreases by 39% when the S111 Suzlon turbine is changed from the upwind configuration into a downwind turbine. In the backward whirl mode the damping increases 18% when the S111 Suzlon turbine is changed from an upwind configuration into a downwind configuration. Differences in out-of-plane displacements cause the main difference in damping between the two turbine configurations and the two modes. As the eigenfrequency of the edgewise forward whirl mode is closer to the second yaw frequency the forward whirl mode will show a higher difference in damping between the configurations. The difference in damping of the foreward whirl mode dominates therefore the over all change in damping when the upwind configuration is changed into the downwind configuration, as well as the difference in extreme and fatigue loads.

2 Methods

In this study two different attempts are used to investigate the difference in edgewise damping between an upwind configuration and a downwind configuration. Firstly, the edgewise damping of the full turbine is calculated from HAWC2 timeseries for upwind and downwind configuration with the full turbine flexibility, called the fully flexible (FF) configurations. Further the edgewise damping is estimated for turbine configurations with reduced flexibility. The flexibility is reduced by increasing the stiffness of certain turbine components significantly. The turbine flexibility is reduced to the rotor flexibility and tower torsional flexibility, as this configuration resembles the difference in edgewise damping with the minimum degrees of freedom. The configurations with reduced flexibility are called the upwind RTT (rotor and tower torsion) and the downwind RTT configuration. Secondly, the influence of shaft length, cone angle and tower torsional stiffness on the edgewise damping of the upwind RTT and downwind RTT configuration are studied by parametric variation. the influence of the shaft length is investigated in a range of -30% and +100%, the cone angle, coning away from the tower from 0° to 7.5°, and the tower torsional stiffness in a range of ± 80%. Table 1 shows a summary of all the configurations used in the study and the investigated parameter variation.

The study is based on a Suzlon S111 2.1MW, class IIIA turbine with a rotor diameter of 112m and 90m tubular tower height. The turbine is pitch regulated and operating at variable rotor speed below rated power. The operational range is from 4ms^{-1} to 21ms^{-1} and rated wind speed is 9.5ms^{-1}. Blade prebend and shaft tilt are neglected in the study to reduce coupling terms between in-plane and out-of plane modes. The cone angle is neglected other than for the parameter study for the same reason. The turbine is assembled as a downwind configuration by shifting the rotor behind the tower and yawing the shaft by 180°.

https://doi.org/10.5194/wes-2019-88
Preprint. Discussion started: 2 December 2019

eawe european academy of wind energy
Open Access WIND ENERGY SCIENCE DISCUSSIONS

2.1 Damping estimation from timeseries

The damping of the turbine edgewise modes is estimated from HAWC2 (Madsen et al. (2019) (Version 12.7)) timeseries. Alternatively, HAWCStab2 (Hansen (2004)) could be used to solve a linearised stability model around the non-linear deflected steady state. In doing so, the eigenfrequencies, damping and modeshapes can be obtained directly by solving an eigenvalue problem of the linearised system. However, due to unresolved issues with respect to modelling downwind turbines in HAWC-Stab2 (which has only been used and tested in the traditional upwind context) it was considered outside the scope of this investigation to address those challenges. The turbine configurations from Tab. 1 are subject to a uniform wind field without turbulence, wind shear or tower shadow, to reduce the noise in the timeseries. The gravity is set to zero to avoid excitation with the rotational frequency on the edgewise signal. The controller is exchanged by a simple setting of pitch angle and rotational speed according to the wind speed at hub height to allow for a slow wind speed increase to avoid other modal frequencies than the excited frequencies in the timeseries. A long run-in time is used to assure that the steady state positions of the turbine are reached and the noise from the run-in does not disturb the vibration signal. The foreward and backward edgewise whirl mode are excited with a harmonic force at the blade at around r/R=75% radius with the blade edgewise frequency. A time shift of 1/3 of the vibration period between the excitation forces on the three blades assures that either the forward whirl mode or the backward whirl mode are excited. The foreward whirl mode is exited with the blade order 3-2-1, as the blades are named in the tower passing order seen from the front. The backward whirl mode is excited with the blade excitation order 1-2-3. After the excitation has stopped, 10 seconds of the timeseries signal are neglected and 50 seconds are used for estimation of damping of the edgewise modes. It has been tested with the aeroelastic modal analysis tool HAWCStab2 (Hansen (2004)) that the trends over wind speed as well as trends for the difference of damping between the configurations are captured correctly for investigations of qualitative differences.

For a primary damping estimation the damping coefficient for a single airfoil as described by Hansen (2007) is calculated. The damping coefficient is calculated from simulated steady state values of the airfoil coefficients and angle of attack at 9m/s, -3° pitch angle and r/R=75% rotor radius.

From the timeseries the logarithmic damping decrement of the edgewise modes is extracted. For the estimation of damping the decaying displacement signal of the 3 blades at r/R=75% radius is used. The logarithmic damping decrement δ is calculated via

$$\delta = \frac{1}{N} ln \frac{x(t)}{x(t+NT)} \tag{1}$$

where N is the number of positive successive peaks, $x(t)$ is the edgewise displacement amplitude of the first peak and $x(t+NT)$ is the amplitude of the Nth peak at N vibration periods T after the first peak. The logarithmic damping decrement is converted to the damping ratio ζ

$$\zeta = \frac{1}{\sqrt{1+\left(\frac{2\pi}{\delta}\right)^2}} \tag{2}$$

The damping ratio is estimated from simulations for the backward and foreward whirling mode of the fully flexible (FF) configurations as well as the upwind RTT and the downwind RTT configuration over the range of operational wind speeds.

https://doi.org/10.5194/wes-2019-88
Preprint. Discussion started: 2 December 2019

WIND ENERGY SCIENCE DISCUSSIONS

2.2 Coleman transformed timeseries

By transforming the velocities and displacements to multiblade- or coleman-coordinates (Bir (2008)) the difference in damping for the timeseries at 9ms^{-1} can be further investigated. For the r/R=75% airfoil section of the upwind RTT and downwind RTT configuration the velocities and displacements are transformed to coleman-coordinates such that the components due to the blade self-motion as well as the motion of the substructure can be considered. The later is the motion of the non-deflected blade due to the tower torsion.

The modal displacement and modal velocities of the r/R=75% rotor position in the coleman coordinates have been calculated via fft-analysis in Matlab. In order to keep a global reference phase for all signals between the different fft-calculations the fft-analysis is once done on the original signal and once on the signal where the azimuth position with a factor of 1/1000 is added. From the comparison of the phase of the original signal and the phase of the signal including the azimuth position all signals can be referenced to the phase of the global azimuth position. This guaranties, that the phasing between the substructure and the rotor modes are consistent between several fft-calculations.

3 Results

The result section presents the estimated edgewise damping as a function of wind speed for the fully flexible up-and downwind FF configuration as well as the up-and downwind RTT configuration. Further the out-of-plane displacement of the edgewise modes is shown to be the reason for the difference in damping. Finally the damping for the parameter variation for shaft length, cone angle and tower torsional stiffness is presented.

3.1 Edgewise damping over wind speed estimated from timeseries

Figure 1 shows the estimated normalized damping ratio as a function of wind speed for the backward (Fig. 1 (a)) and foreward whirl mode (Fig. 1 (b)) for the fully flexible up- and downwind FF configuration, as well as the upwind RTT and downwind RTT configuration. The figure further shows the difference in damping between the upwind configuration RTT and the other configurations (Fig. 1 (c) and (d)).

The figure shows that both edgewise modes in both configurations are positively damped. The damping ratio increases from cut-in wind speed to a local maximum at rated wind speed. After decreasing for wind speeds between rated wind speed and wind speeds around 14ms^{-1}, a damping increase for wind speeds higher than 14ms^{-1} is observed. In the backward whirl mode (Fig. 1 (a)) the downwind configurations are subject to higher edgewise damping than the respective upwind configurations. The difference is approximately 18% for the RTT configurations (see Fig. 1 (c)). In the foreward whirling mode (Fig. 1 (b)) the two downwind configurations are subject to significantly lower edgewise damping than the respective upwind configurations over the investigated wind speed range. The difference in edgewise damping is largest around rated wind speed, where the damping is approximately 39% lower in the downwind RTT configuration than the upwind RTT configuration (Fig. 1 (d)).
For the upwind configurations the foreward whirl mode (Fig. 1 (b)) is significantly higher damped than the backward whirl

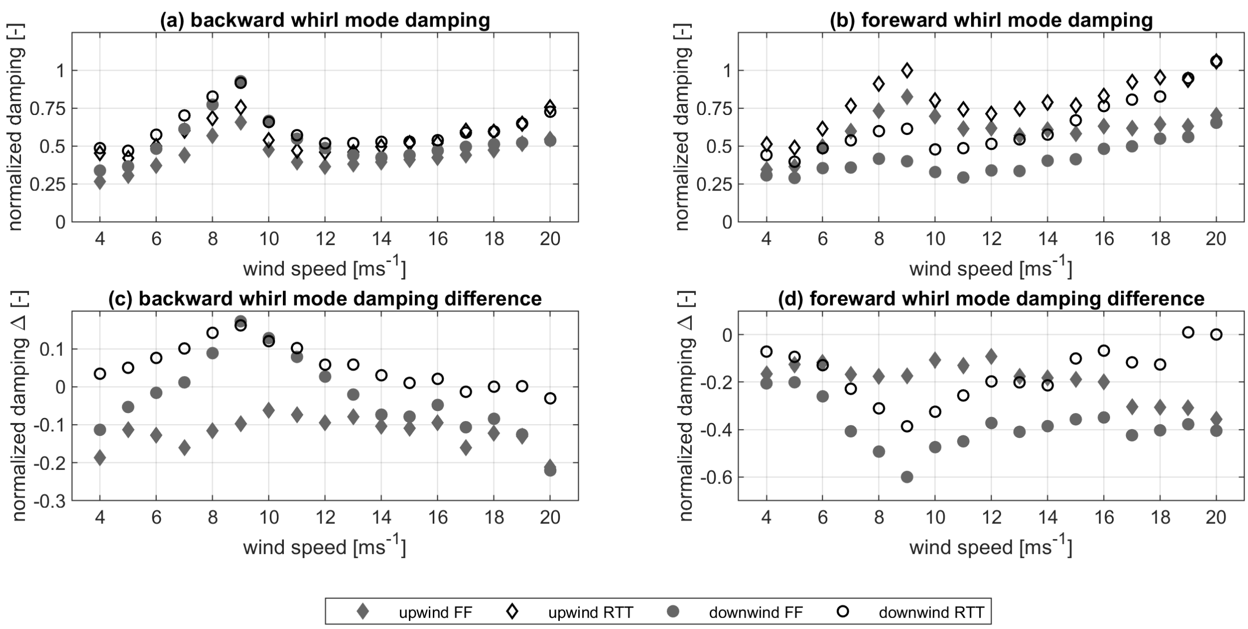

Figure 1. Normalized damping ratio as function of wind speed for the back whirl mode (a) and the foreward whirl mode (b) for the upwind RTT and the downwind RTT configuration and the fully flexible FF configurations, as well as the difference in damping to the damping to the upwind RTT configuration in the backward whirl mode (c) and the foreward whirl mode (d). The damping as well as the damping difference are normalized with the damping of the upwind RTT configuration at 9 ms^{-1} of the foreward whirl mode.

mode (Fig. 1 (a)), as also shown by Hansen (2003), since the foreward whirl mode has a higher out-of-plane component of the mode shape than the backward whirl mode. When the tower flexibility is removed from the model or when the aerodynamic forces are not present, the damping of both foreward and backward modes are identical. This indicates that the difference in damping is driven by the interaction of the aerodynamic forces on the rotor with the tower torsional motion.

3.2 Modal displacement effects on edgewise damping

The observed difference in normalized edgewise damping between the upwind and the downwind configuration presented in Fig. 1 can not be explained with the analytical airfoil in-plane damping coefficient derived by Hansen (2007). There is no difference in the coefficient, since the steady state values of the airfoil coefficients and the according slopes are the same. Further no difference in the in-plane velocities could be found. Thus, the difference in edgewise damping has to be explained by the out-of-plane displacements in the modes for the different turbine configurations. The out-of-plane components can be either due to the flap component in the edgewise modes, or due to the tower torsion that rotates the blades out of the reference plane. This section shows

– higher out-of-plane displacement gives higher edgewise damping

https://doi.org/10.5194/wes-2019-88
Preprint. Discussion started: 2 December 2019

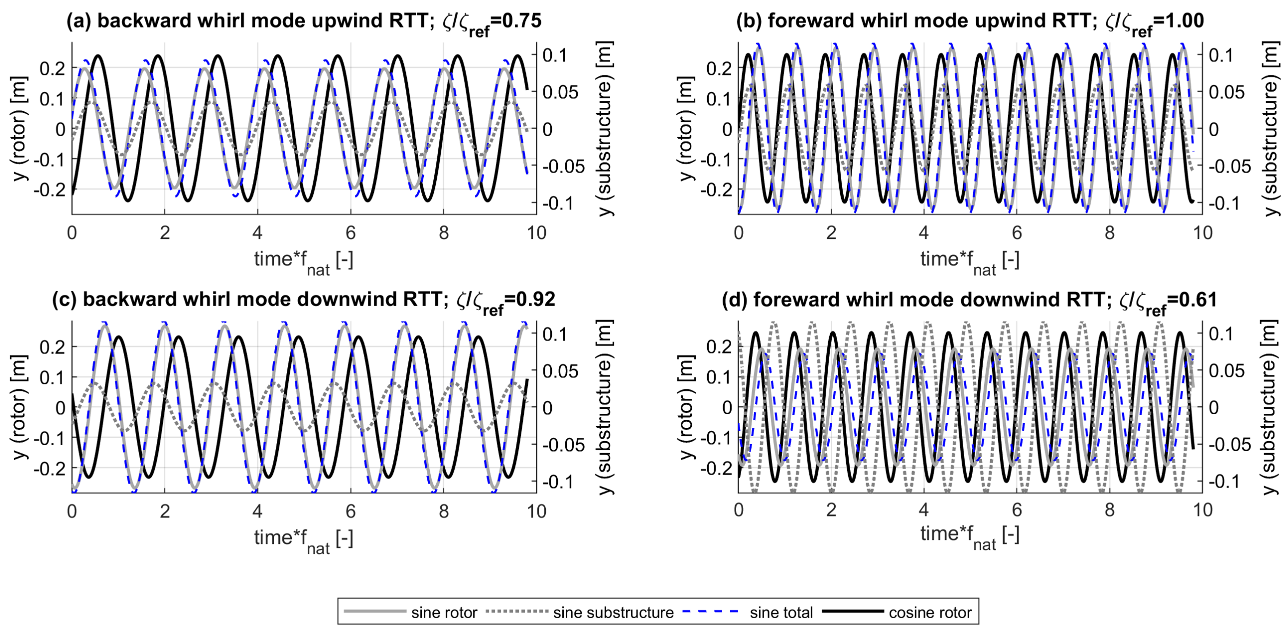

Figure 2. Modal out-of-plane displacements at $9\mathrm{ms}^{-1}$ for the backward whirl mode ((a), (c)) and foreward whirl mode ((b), (d)) of the upwind RTT ((a), (b)) and downwind RTT configuration ((c), (d)). The time axis is normalized with the blade edgewise natural frequency.

- difference in forcing due to configuration gives difference in modal phases
- difference in modal phases gives difference in damping

Figure 2 shows the out-of-plane displacements of the sine and cosine components of the rotor, as well as the sine displacement component due to the substructure, e.g. the tower torsion, for the backward whirl mode (Fig. 2 (a) and (c)) and the foreward whirl mode (Fig. 2 (b) and (d)) of the upwind RTT and the downwind RTT configuration.

The figure shows that there generally is a phase shift between the sine component of the out-of plane displacement between the substructure and the rotor. Adding the two signals leads to the total sine component of the out-of plane displacement with the same frequency, but a different amplitude and phase. Only in the foreward whirl mode of the downwind RTT configuration, which is also the mode with the over all lowest damping, the total out-of-plane displacement is reduced due to the tower torsional displacement (Fig. 2 (d)). Generally, the main contribution to the out-of-plane displacement is due to the rotor self-motion. The foreward whirl mode (Fig. 2 (b) and (d)) shows generally higher out-of-plane displacements of to the substructure than the respective backward whirl mode (Fig. 2 (a) and (c)), as the natural frequency of the foreward whirl mode is closer to the natural frequency of the second yaw mode. The natural frequencies of the modes are the same for the upwind and the downwind configuration.

The interaction of the rotor and the tower causing a higher sine out-of-plane displacement of the rotor leading to higher

https://doi.org/10.5194/wes-2019-88
Preprint. Discussion started: 2 December 2019

damping in the foreward whirl mode of the upwind RTT configuration (2 (b)) and the backward whirl mode in the downwind RTT configuration (2 (c)) than respective modes with lower sine out-of-plane displacements. The foreward whirl mode of the upwind RTT configuration (2 (b)) further shows a 5% higher out-of-plane cosine component of rotor displacement than the downwind RTT configuration in the backward whirl mode (2 (c)), which explains the remaining difference in damping between the two turbine configurations.

The higher sine component of the rotor out-of-plane displacement can not be associated with the frequency of the second yaw mode, as this does not hold true for the backward whirl mode of the downwind configuration (Fig. 2 (c)). The higher out-of-plane rotor displacement in the sine component is observed to come with a sine component of the substructure out-of-plane displacement that is lagging the respective rotor displacement (Fig. 2 (b) and (c)). If the sine component of the of the out-of-plane displacement of the substructure is leading the respective rotor displacement the sine component of the out-of-plane rotor displacement is lower (Fig. 2 (a) and (d)).

Also the in-plane motion of the rotor (not shown here) is subject to a sine component lagging the cosine component in the backward whirl mode and a sine component leading the cosine component in the foreward whirl mode. The modal velocities cause aerodynamic forces. Inherently to the whirl modes the aerodynamic in-plane forces at the hub sum up to a non-zero total in-plane force. With the arm of the shaft length this force causes a yaw loading. Depending on the placement of the rotor relative to the yaw center a positive in-plane cosine force at the hub causes a positive yaw loading (upwind configuration) or a negative yaw loading (downwind configuration). The response of the tower, e.g. the out-of-plane substructure sine component of displacement is therefore either lagging the the out-of-plane sine component of the rotor displacement, as in the foreward whirl mode of the upwind RTT configuration (2 (b)) and the backward whirl mode of the downwind RTT configuration (2 (c)) or the sine component of the substructure out-of-plane displacement is leading the rotor sine out-of-plane displacement (upwind RTT configuration, backward whirl mode, Fig. 2 (a) and downwind RTT configuration, foreward whirl mode, Fig. 2 (d)).

Form this analysis it can be seen that the difference in edgewise damping is due to a difference in out-of-plane motion. The main contributor is the higher rotor out-of-plane motion associated with a favorable phasing between the out-of-plane motion of the substructure and the out-of-plane sine component of the rotor motion. It will therefore be expected from the analysis described in the previous paragraphs, that the edgewise damping can be increased by an increase of the yaw loading, if the substructure displacement is lagging the sine out-of-plane displacement of the rotor. The damping is on the other hand expected to decrease with an increased yaw loading if the substructure displacement is leading the sine out-of-plane displacement of the rotor. Increasing the shaft length is expected to increase the damping of the edgewise foreward whirl mode in the upwind configuration as well as in the backward whirl mode of the downwind configuration. In the backward whirl mode of the upwind configuration and the foreward whirl mode of the downwind configuration an increase in shaft length is expected to decrease the edgewise damping.

https://doi.org/10.5194/wes-2019-88
Preprint. Discussion started: 2 December 2019

3.3 Parameter variation: shaft length

Figure 3 shows the normalized edgewise damping values of the backward whirl mode (Fig. 3 (a) and (c)) and foreward whirl mode (Fig. 3 (b) and (d)) for the upwind RTT configuration (Fig. 3 (a) and (b)) and the downwind RTT configuration (Fig. 3 (c) and (d)) as a function of wind speed and shaft length factor. The figure shows that the normalized edgewise damping of

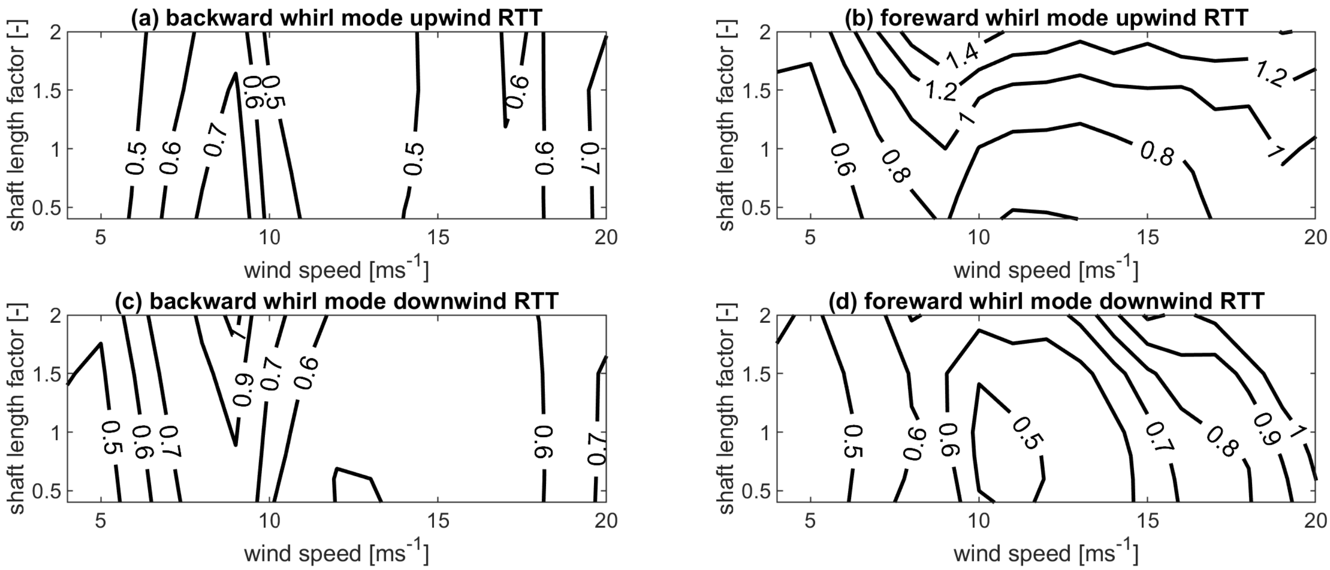

Figure 3. Normalized edgewise damping ratio as a function of wind speeds and shaft length factor for the backward whirl mode ((a) and (c)) and the foreward whirl mode ((b) and (d)), for the upwind RTT configuration ((a) and (b)) and the downwind RTT configuration ((c) and (d)). The edgewise damping is normalized with the damping value of foreward whirl mode in the upwind RTT configuration at a shaft length factor of 1 at 9ms^{-1}.

the backward whirling mode in the upwind RTT configuration decreases with the increasing shaft length (Fig. 3 (a)). In the downwind RTT configuration on the other hand the normalized edgewise damping increases with the increasing shaft length in the backward whirl mode (Fig. 3 (c)). The effect is strongest pronounced around rated wind speed. In the forward whirl mode of the upwind RTT configuration the normalized edgewise damping increases with the increasing shaft length (Fig. 3 (b)). The normalized edgewise damping of the downwind RTT configuration on the other hand hardly changes with the increasing shaft length for wind speeds close to rated wind speed (Fig. 3 (d)).

For a shaft length factor of 2 and at 9ms^{-1} the out-of-plane displacements (see appendix Fig. A1) have been compared to the displacements for a shaft length factor of 1 at 9ms^{-1} (Fig. 2). Both turbine configurations in the backward whirl mode and also the upwind RTT configuration in the foreward whirl mode show the expected dependency on the shaft length according to Sect. 3.2 around rated wind speed: the normalized edgewise damping of the backward whirl mode of the downwind RTT configuration and the normalized edgewise damping of the foreward whirl mode in the upwind RTT configuration are increas-

https://doi.org/10.5194/wes-2019-88
Preprint. Discussion started: 2 December 2019

eawe european academy of wind energy
Open Access WIND ENERGY SCIENCE DISCUSSIONS

ing due to higher out-of-plane displacements in the rotor sine components. In the backward whirl mode of the upwind RTT configuration a decrease of the sine component of the out-of-plane rotor displacements can be observed. Also for the downwind RTT configuration in the foreward whirl mode the expected decrease of out-of-plane sine component of rotor displacement can be observed. However, an increase of the cosine out-of-plane displacements of the rotor can also be seen. The combination of the out-of-plane displacements leads to the effect that hardly any difference in edgewise damping can be observed at around rated wind speed for the foreward whirl mode of the downwind RTT configuration.

3.4 Parameter variation: cone angle

Figure 4 shows the normalized edgewise damping for the backward whirl mode (Fig. 4 (a) and (c)) and the forward whirl mode (Fig. 4 (b) and (d)) in the upwind RTT (Fig. 4 (a) and (b)) and the downwind RTT configuration (Fig. 4 (c) and (d)) as a function of cone angle and wind speed.

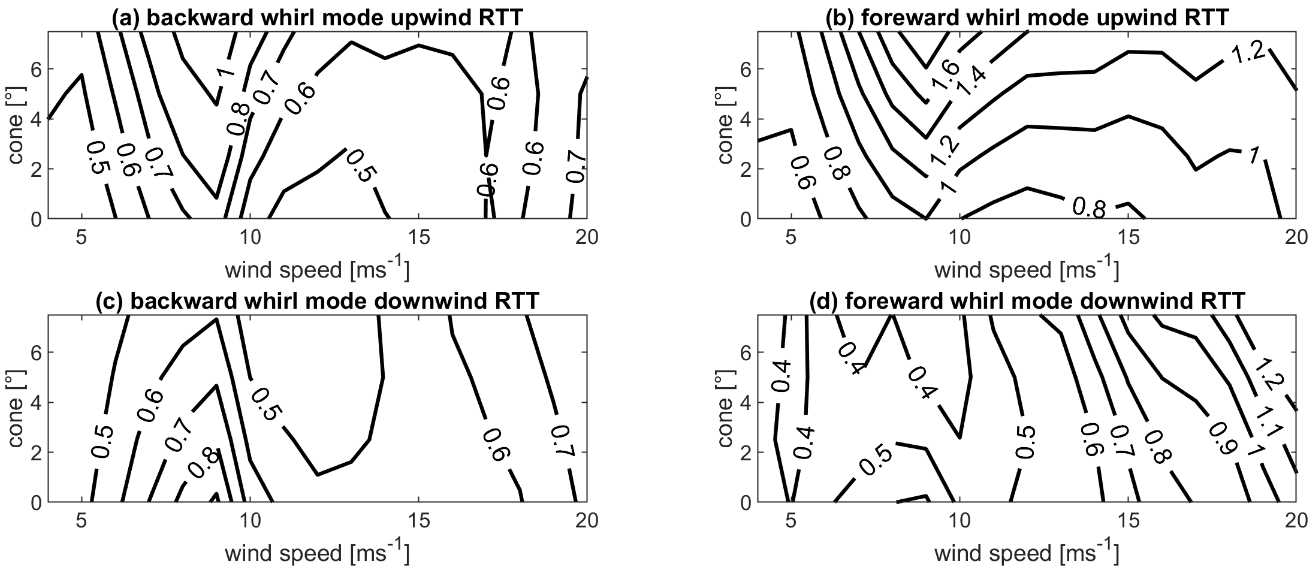

Figure 4. Normalized edgewise damping as a function wind speeds and cone angle for the backward whirl mode ((a) and (c)) and the foreward whirl mode ((b) and (d)), for the upwind RTT configuration ((a) and (b)) and the downwind RTT configuration ((c) and (d)). The damping is normalized with the damping value of foreward whirl mode in the upwind configuration at 0° at 9 ms^{-1}.

The figure shows that the edgewise damping of both modes increases with increasing cone angle in the upwind RTT configuration (Fig. 4 (a) and (b)). In the downwind RTT configuration the edgewise damping decreases with increasing cone angle for wind speeds around rated wind speed (Fig. 4 (c) and (d)).

Introducing the cone angle has several effects. On the one hand, the cone angle changes the steady state values of the airfoil coefficients and therefore the estimated analytical damping coefficient by Hansen (2007): The blades deflect against the coning direction in the upwind RTT configuration, while the blades deflect in the same direction as the cone direction in the down-

https://doi.org/10.5194/wes-2019-88
Preprint. Discussion started: 2 December 2019

wind RTT configuration. The analytical damping coefficient of the r/R=75% airfoil at 9ms^{-1} has decreased by 33% in the upwind RTT configuration when a cone angle of 7.5° is introduced. The analytical damping coefficient of the r/R=75% airfoil at 9ms^{-1} has increased by 38% in the downwind RTT configuration when a cone angle of 7.5° is introduced. On the other hand, the cone angle also changes the coupling between the in-plane loading and the tower torsion as the distance between the yaw axis and the outboard airfoils is increased. Comparing the displacements at 9ms^{-1} at a cone angle of 7.5° (Fig. A2) with the out-of-plane displacements at 9ms^{-1} without cone angle (Fig. 2) shows only very little changes in the rotor sine components of the out-of-plane displacements. However, the downwind RTT configuration shows a significant decrease in the cosine component of the out-of-plane rotor displacements, while the upwind RTT configuration shows a significant increase in the cosine out-of-plane rotor displacements when the cone angle of 7.5° is introduced. The changes in the cosine out-of-plane rotor displacement dominate the change in normalized edgewise damping.

3.5 Parameter variation: tower torsion

Figure 5 shows the normalized edgewise damping for the backward whirl mode (Fig. 5 (a) and (d)) and foreward whirl mode (Fig. 5 (b) and (c)) of the upwind RTT (Fig. 5 (a) and (b)) and downwind RTT configuration (Fig. 5 (c) and (d)) as a function wind speed and tower torsion stiffness factor.

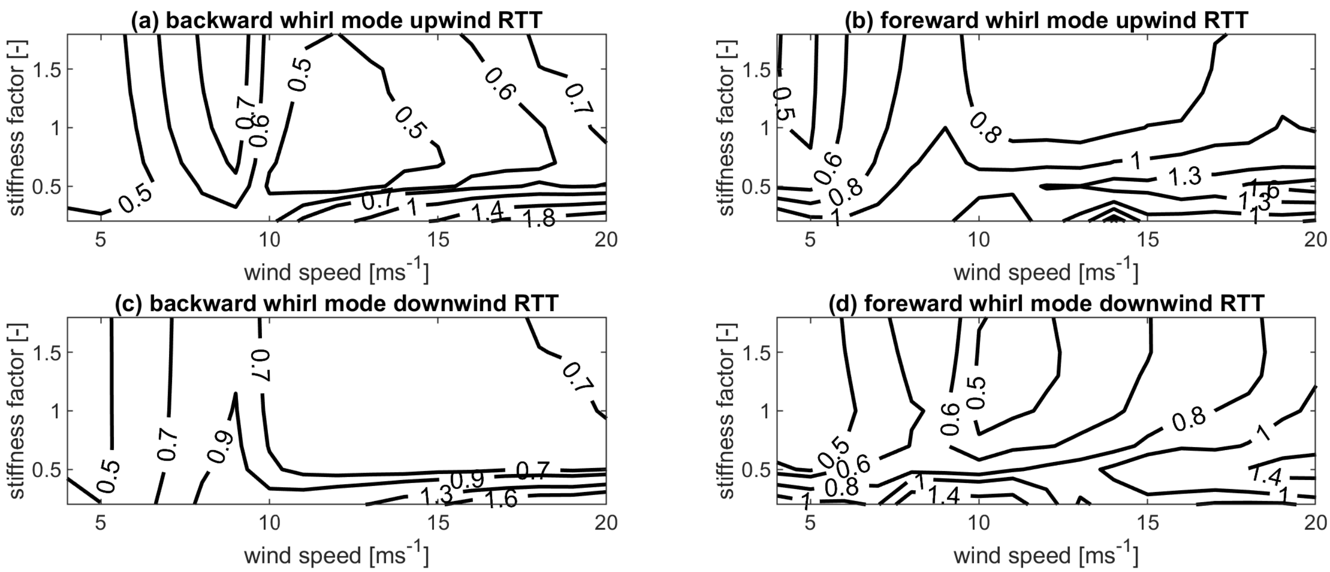

Figure 5. Normalized edgewise damping as a function of wind speeds and tower torsion stiffness factor for the backward whirl mode ((a) and (c)) and the foreward whirl mode ((b) and (d)), for the upwind RTT configuration ((a) and (b)) and the downwind RTT configuration ((c) and (d)). The damping is normalized with the damping value of foreward whirl mode in the upwind RTT configuration at a tower torsion stiffness factor of 1 at 9 ms^{-1}.

https://doi.org/10.5194/wes-2019-88
Preprint. Discussion started: 2 December 2019

While the normalized edgewise damping is increasing in the backward whirl mode of the upwind RTT configuration with the increasing tower torsional stiffness (Fig. 5 (a)), the normalized edgewise damping of the backward whirl mode of the downwind RTT configuration (Fig. 5 (c)) is decreasing with increasing tower torsional stiffness at around rated wind speed. For high wind speeds and a stiffness factors lower than 0.5 the edgewise damping of the backward whirl mode increases drastically with the decreasing tower torsional stiffness for both configurations. In the foreward whirl mode the normalized edgewise damping generally decreases in both configurations with an increasing tower torsional stiffness (Fig. 5 (b) and (d)). Both configurations in the foreward whirl mode show an area at around cut-out wind speeds at a stiffness factor at around 0.5, where a local maximum of normalized edgewise damping is reached.

Comparing Fig. A3 with Fig.2 shows that a decrease of tower torsional stiffness to a factor of 0.2 at 9 ms^{-1} increases generally the out-of-plane displacements associated with the substructure. Further, phasing between the substructure and rotor out-of-plane displacement as well as the rotor associated out-of-plane displacement is changing. Over all, only the upwind RTT configuration in the backward whirl mode does not benefit from the decrease in the tower torsional stiffness in the out-of-plane displacements at 9 ms^{-1}. At high wind speeds the effect of the frequency placement can be observed. As the tower torsional stiffness decreases below a factor of around 0.5 the second yaw frequency crosses the edgewise foreward whirl mode frequency and moves closer to the edgewise backward whirl mode frequency. Thus, the highest damping at high wind speeds is observed at at stiffness factor of around 0.5 for high wind speeds.

4 Summary

In this article the change in edgewise damping when an upwind wind turbine is converted into a downwind configuration has been investigated on the example of a simplified version of the commercial Suzlon S111 2.1MW wind turbine. The edgewise forward whirl mode has been shown to decrease in damping as the upwind configuration is changed into the downwind configuration. The edgewise backward whirl mode on the other hand has been seen to increase in damping when the upwind configuration is changed into a downwind configuration. The interaction with the aerodynamic forces, the rotor and tower torsional motion have been shown to create a difference in out-of-plane displacement. The out-of-plane displacement was seen to cause the observed differences in edgewise damping.

The difference in the out-of plane displacements and therefore damping was shown to increase with an increased shaft length, as the yaw loading from the in-plane cosine shear forces could be increased. An increase in cone has been shown to increase cosine component of the out-of-plane rotor displacements and therefore damping for the upwind configuration, while the increase in cone causes a decrease in cosine component of the out-of-plane displacements and damping in the downwind configuration. A decrease in tower torsional stiffness has been seen to increase the damping from a favourable placement of natural frequencies relative to each other, as long as the rotor and substructure out-of-plane displacement do not counteract each other due to phase differences.

https://doi.org/10.5194/wes-2019-88
Preprint. Discussion started: 2 December 2019

5 Conclusion and future work

As a decrease in damping increases extreme as well as fatigue loads, the edgewise damping should be included in the design considerations. For the shaft length there would be a trade-off between edgewise damping of the two modes, but also the rotor overhanging moment that has to be carried by the support structure. The consideration of edgewise damping would suggest a higher cone angle for upwind configurations than for downwind configurations. Again, other considerations like tower clearance, flapwise blade root loads and power production compete in the design decision. From an edgewise damping point of view downwind configurations could benefit from towers with lower torsional stiffness. Replacing a tubular tower or the bottom segments of the tubular tower by a lattice structure could significantly increase the overall edgewise damping.

The damping of the first two edgewise whirl modes has been estimated from timeseries where the foreward or backward whirl mode are excited. Using the same model as used for load simulations has the advantage of estimating directly the differences in damping without linearization effects. However, this method will only be able to estimate the damping, if clearly only one mode is excited and only one frequency dominates the spectrum. Further the damping has to be so low, that the peak to peak counting and amplitude detection can be reliably performed. In this study normalized edgewise damping above a normalized damping of 1.8 could not be estimated. This limited effectively the investigated range of the investigated parameter. The edgewise modes are well suited for this method as they are significantly lower damped than other modes. Estimating the damping from an eigenvalue solution would eliminate these limitations.

Future work should investigate further the reason for the different out-of-plane displacement in the mode shapes, especially the differences observed in the cosine components of the out-of-plane displacement. Further the degrees of freedom of the turbine model should be extended to the full flexibility, as additional degrees of freedom are expected to affect the mode shapes, especially the turbine tilting flexibility (tower fore-aft and shaft bending flexibility), or shaft bending and torsional flexibility could influence the edgewise damping.

Data availability. The data is not publicly accessible, since the research is based on a commercial turbine and the data is not available for disclosure by Suzlon.

Appendix: Out-of-plane displacements for parameter variations

The following figures show the out-of-plane displacements of the two edgewise damping modes in the two RTT configurations at 9ms^{-1} for a shaft length factor of 2 (Fig. A1), a cone angle of 7.5° (Fig. A2) and a tower torsional stiffness factor of 0.2 (Fig. A3).

https://doi.org/10.5194/wes-2019-88
Preprint. Discussion started: 2 December 2019

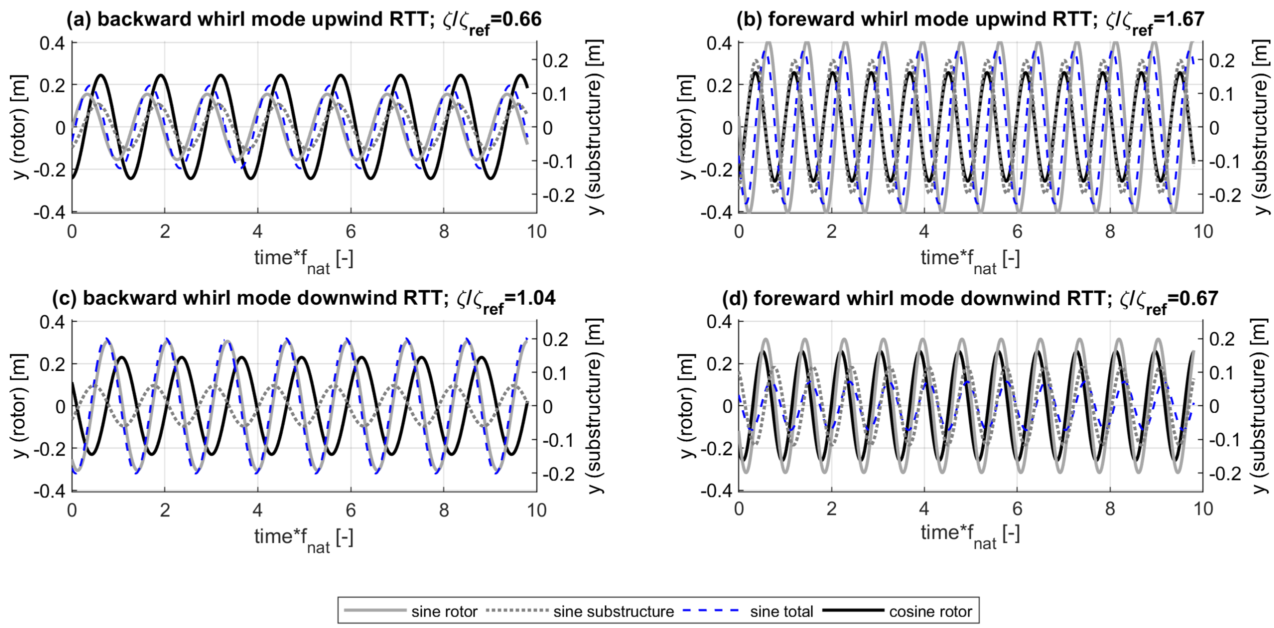

Figure A1. Modal out-of-plane displacements at $9\mathrm{ms}^{-1}$ and a shaft length factor of 2 for the backward whirl mode and foreward whirl mode of the upwind RTT and downwind RTT configuration. The time axis is normalized with the blade edgewise natural frequency.

https://doi.org/10.5194/wes-2019-88
Preprint. Discussion started: 2 December 2019

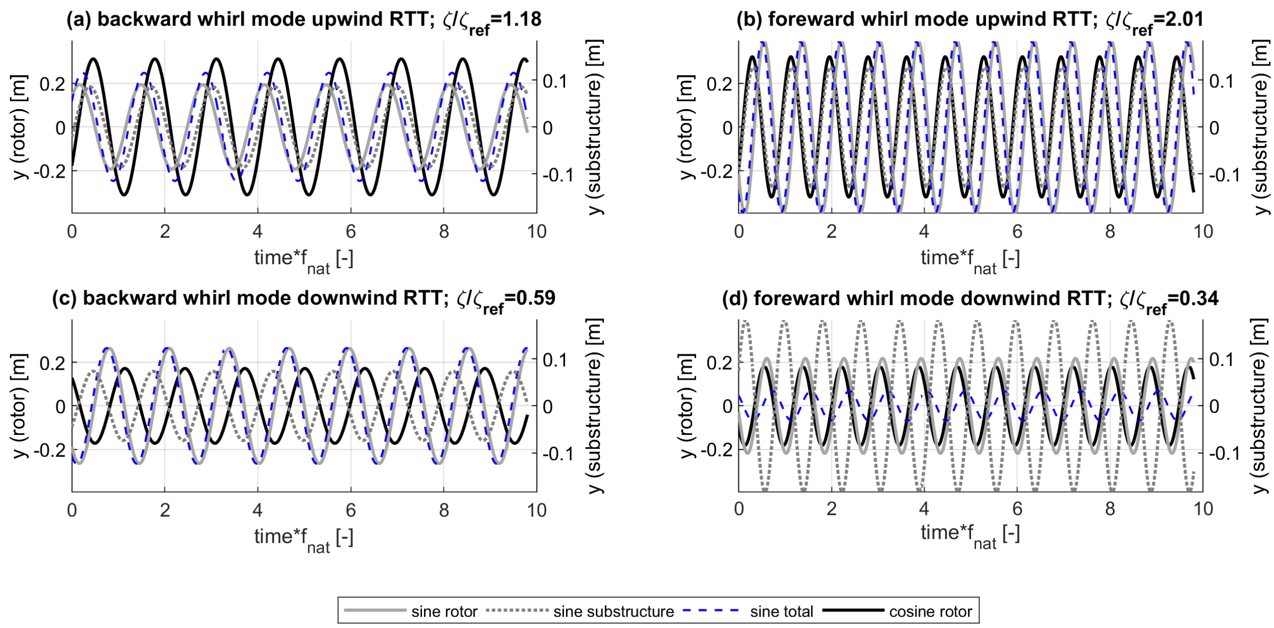

Figure A2. Modal out-of-plane displacements at $9 ms^{-1}$ and a cone angle of 7.5° for the backward whirl mode and foreward whirl mode of the upwind RTT and downwind RTT configuration. The time axis is normalized with the blade edgewise natural frequency.

https://doi.org/10.5194/wes-2019-88
Preprint. Discussion started: 2 December 2019

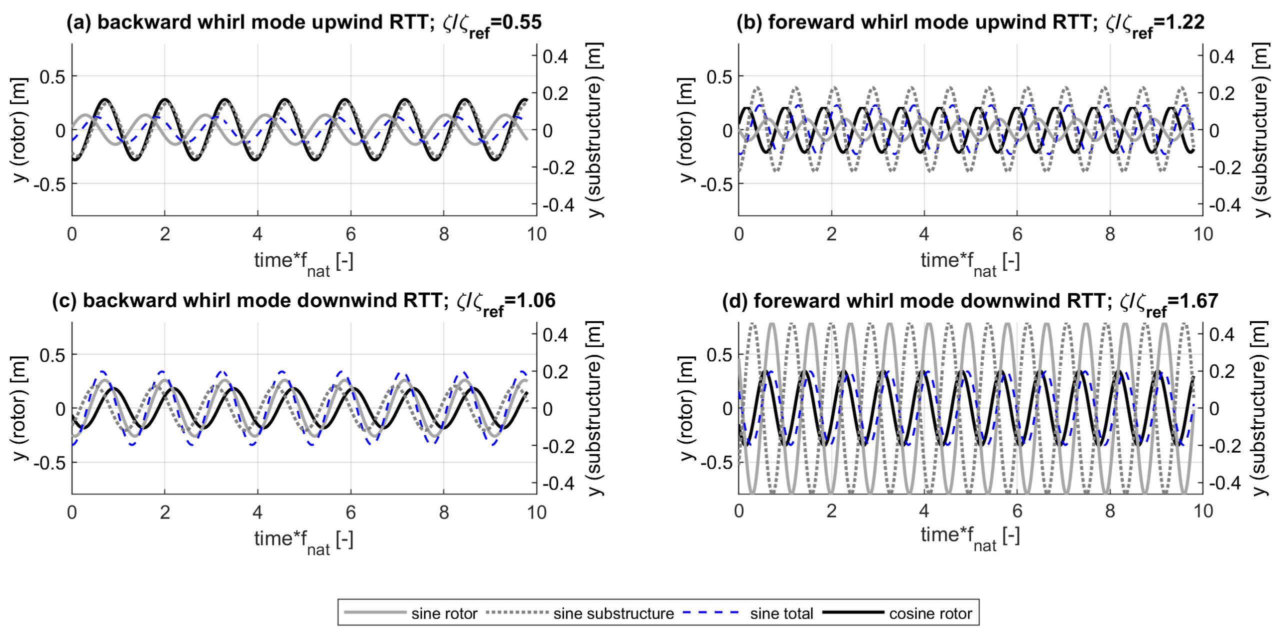

Figure A3. Modal out-of-plane displacements at 9ms^{-1} and a tower torsional stiffness factor of 0.2 for the backward whirl mode and foreward whirl mode of the upwind RTT and downwind RTT configuration. The time axis is normalized with the blade edgewise natural frequency.

https://doi.org/10.5194/wes-2019-88
Preprint. Discussion started: 2 December 2019

Author contributions. GW set-up the models and carried out the calculations. LB and DV revised the models. All authors have interpreted the obtained data. GW prepared the paper with revisions of all co-authors.

Competing interests. This project is an industrial PhD project funded by the Innovation Fund Denmark and Suzlons Blade Science Center. Gesine Wanke is employed at Suzlons Blade Science Center.

https://doi.org/10.5194/wes-2019-88
Preprint. Discussion started: 2 December 2019

References

Bir, G.: Multiblade Coordinate Transformation and Its Application to Wind Turbine Analysis, Report NREL/CP-500-42553, 2008.

Glasgow, J., Miller, D., and Corrigan, R.: Comparison of upwind and downwind rotor operations of the DOE/NASA 100-kW MOD-0 wind turbine, NASA Report; No. TM-8744; p. 225–234, 1981.

Hansen, M. H.: Improved Modal Dynamics of Wind Turbines to Avoid Stall-induced Vibrations, Wind Energy; Vol. 6; p. 179-195, https://doi.org/10.1002/we.79, 2003.

Hansen, M. H.: Aeroelastic Stability Analysis of Wind Turbines Using an Eigenvalue Approach, Wind Energy; Vol. 7; p. 133-143, https://doi.org/10.1002/we116, 2004.

Hansen, M. H.: Aeroelastic instability problems for wind turbines, Wind Energy; Vol. 10; Nr. 6; p. 551-577, https://doi.org/10.1002/we.242, 2007.

Madsen, H. A., Larsen, T. J., Pirrung, G. R., and Zahle, F.: Implementation of the Blade Element Momentum Model on a Polar Grid and its Aeroelastic Load Impact, Wind Energy Science Discussion, https://doi.org/10.5194/wes-2019-53, in review, 2019.

Petersen, J. T., Madsen, H. A., Bjoerck, H. A., Enevoldsen, P., Øye, S., Ganander, H., and Winkelaar, D.: Prediction of dynamic loads and induced vibrations in stall, Risø-Report (Risø-R-1045(EN)), 1998a.

Petersen, J. T., Thomsen, K., and Madsen, H. A.: Local blade whirl and global rotor whirl interaction, Risø-Report (Risø-R-1067(EN)), 1998b.

Reiso, M. and Muskulus, M.: The simultaneous effect of a fairing tower and increased blade flexibility on a downwind mounted rotor, Journal of Renewable and Sustainable Energy; Vol. 5; p. 033106-1–1033106-11, https://doi.org/10.1063/1.4803749, 2013.

Thomsen, K., Petersen, J. T., Nim, E., Øye, S., and Petersen, B.: A Method for Determination of Damping for Edgewise Blade Vibrations, Wind Energy, https://doi.org/10.1002/we.42, 2000.

Wanke, G., Bergami, L., Larsen, T. J., and Hansen, M.: Changes in design driving load cases: Operating an upwind turbine with a downwind rotor configuration, Wind Energy, https://doi.org/10.1002/we.2384, 2019.

Zahle, F., Madsen, H., and Sørensen, N.: Evaluation of tower shadow effects on various wind turbine concepts, Research in Aeroelasticity DTU Report EFP-2007-II; Vol. 1698; p.1–147, 2009.

https://doi.org/10.5194/wes-2019-88
Preprint. Discussion started: 2 December 2019

WIND ENERGY SCIENCE DISCUSSIONS

Table 1. Configurations and parameter variations

configuration/ parameter variation	properties
edgewise damping estimation	
all configurations	no tilt, no cone, no prebend
	simplified controller, no gravity, uniform inflow
	(no turbulence, no sheer, no veer, no inclination angle)
upwind FF	upwind, all degrees of freedom (fully flexible)
downwind FF	downwind, all degrees of freedom (fully flexible)
upwind RTT	upwind, rotor flexibility, tower torsion flexibility
downwind RTT	downwind, rotor flexibility, tower torsion flexibility
parameter variation	
shaft length	up- and downwind RTT configuration
	shaft length variation: -30% to +100%
cone angle	up- and downwind RTT configuration
	cone angle variation: $0°$ to $7.5°$ (away from tower)
tower torsional stiffness	up- and downwind RTT configuration
	torsional stiffness factor variation $\pm$ 80%